AJNR

Extraneous lipid contamination in single-volume proton MR spectroscopy: phantom and human studies.

L Kwock, M A Brown and M Castillo

AJNR Am J Neuroradiol 1997, 18 (7) 1349-1357
http://www.ajnr.org/content/18/7/1349

Extraneous Lipid Contamination in Single-Volume Proton MR Spectroscopy: Phantom and Human Studies

Lester Kwock, Mark A. Brown, and Mauricio Castillo

PURPOSE: To determine the degree of extraneous lipid contamination in defined volumes of interest studied with single-volume proton MR spectroscopy. **METHODS:** Single-volume proton MR spectroscopy was performed on a fat/water phantom and in three volunteers using the stimulated-echo acquisition mode (STEAM) and point-resolved spectroscopy (PRESS) localization methods. Three different volumes of interest (8, 27, and 64 cm^3) were examined at echo times of 20, 135, and 270 for the STEAM sequences and 135 and 270 for the PRESS acquisitions in both the phantom and the volunteers (volumes of interest were placed adjacent to but not encompassing fat-containing structures, such as the scalp and retroorbital fat). The degree of lipid contamination was then correlated with measurements of the section profiles. **RESULTS:** The PRESS method resulted in less extraneous lipid contamination in both phantom and volunteer studies. The STEAM method had the highest level of lipid contamination signal in phantom and human studies. In the volunteers, volumes of interest abutting fat-containing structures obtained with PRESS or STEAM sequences showed no lipid contamination. However, the STEAM sequences showed lipid signal in the volume of interest adjacent to orbital fat whereas the PRESS sequences did not. These observations are supported by the section profile studies, which showed that the actual volume excited by the STEAM sequence was 7% to 32% larger than that originally selected, while with PRESS the actual excited volume was 12% to 16% smaller than that originally selected. **CONCLUSION:** In our MR unit, short-echo-time STEAM sequences (≤135 milliseconds) resulted in extraneous lipid contamination in phantom and human studies adjacent to the orbits. PRESS sequences showed no lipid contamination in volumes abutting fat structures in phantoms or humans. These results correlated closely with the configuration of the section profiles. Although these findings might be dependent on the MR unit used, our study could help determine extraneous lipid contamination for other MR units.

Index terms: Brain, magnetic resonance; Magnetic resonance, artifacts; Magnetic resonance, spectroscopy

AJNR Am J Neuroradiol 18:1349–1357, August 1997

Structures with a high concentration of lipids, such as subcutaneous fat and retroorbital spaces, can introduce contamination into brain magnetic resonance (MR) spectra. Even small amounts of extraneous fat can cause fairly intense proton lipid signals. This tends to be problematic in multivolume spectroscopic MR imaging of the brain, as the signal from extraneous fat may be one to two orders of magnitude greater than the proton metabolite resonances of interest (1). Extraneous fat contamination may result from the fact that in MR spectroscopic imaging, data sampling in k-space is obtained by using only a limited number of sample points in the spatial dimension. Fourier transformation of these truncated sample points leads to Gibbs artifacts and associated lipid signal contamination (1). In single-volume MR spectroscopy, extraneous lipid contamination depends primarily on the characteristics of the slice-selection radio frequency pulse used (2). These pulses are frequency selective and nor-

Received September 13, 1996; accepted after revision February 24, 1997.

From the Department of Radiology, University of North Carolina School of Medicine, Chapel Hill (L.K., M.C.), and Siemens Medical Systems, Training and Development Center, Cary, NC (M.A.B.).

Address reprint requests to M. Castillo, MD, Department of Radiology, CB 7510, University of North Carolina, Chapel Hill, NC 27599.

AJNR 18:1349–1357, Aug 1997 0195-6108/97/1807–1349

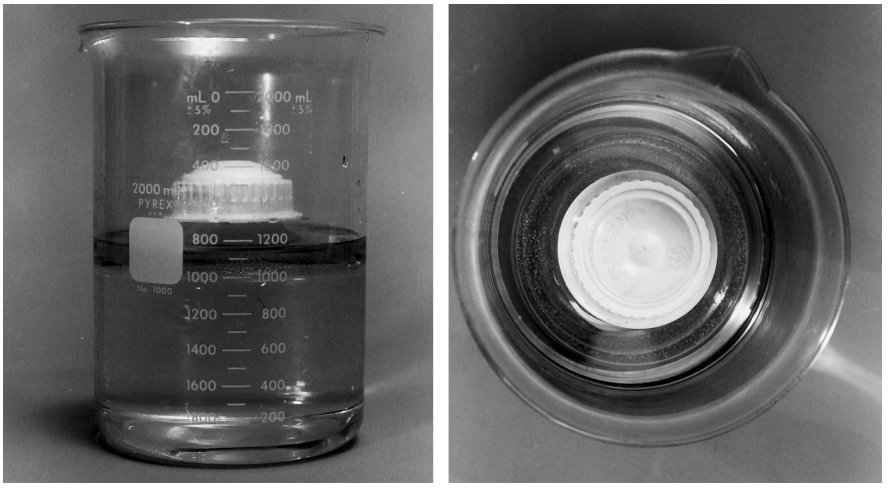

Fig 1. Photographs of the phantom.

A, Frontal view of the phantom shows a 1000-mL glass beaker filled with commercial vegetable oil. The second component is a polystyrene flask filled with a solution containing metabolites similar to those found in the brain.

B, View from above shows the polystyrene flask to be completely surrounded by vegetable oil.

mally truncated sinc functions. Sinc pulses are formed by mixing a sinc function (sin t/t) with a Hanning function in the time domain and then truncating the resulting function to adjust the range of the frequency domain to be excited. Truncation of the sinc function leads to nonrectangular slice-selection profiles and side lobes in the frequency domain pulse, which may excite nuclei outside the defined volume of interest.

Our purpose was to determine the presence of extraneous lipid contamination in two commonly used single-volume localization methods and its relation to varying echo times (TEs), voxel sizes, and section profiles. Experiments were conducted with the use of a phantom of our own design and with human volunteers.

Materials and Methods

Proton MR Spectroscopy

All studies were performed on a Siemens 1.5-T Magnetom SP4000 unit (Siemens Medical Systems, Iselin, NJ) equipped with a circularly polarized transmit/receive head coil. Voxel placement was achieved by using an axial T1-weighted image (500/15/1 [repetition time/TE/excitations]) of the phantom and three axial images of the volunteers (one each at the skull base, midorbit, and centrum semiovale). Localized proton MR spectra of each volume of interest were obtained with either stimulated-echo acquisition mode (STEAM) or point-resolved spectroscopy (PRESS) sequences provided by the manufacturer (3, 4). For STEAM sequences, TEs of 20, 135, and 270 were used for phantom and human studies. For the PRESS method, TEs of 135 and 270 were used for phantom and human studies. Volumes for the STEAM and PRESS methods were $2 \times 2 \times 2$ cm^3, $3 \times 3 \times 3$ cm^3, and $4 \times 4 \times 4$ cm^3 for phantom studies and $2 \times 2 \times 2$ cm^3 and $3 \times 3 \times 3$ cm^3 for human studies. A repetition time of 1600 was used for both STEAM and PRESS methods and 128 scans were averaged for each volume of interest. A narrow bandwidth (60 Hz) generated water-suppression gaussian pulse was used for all sequences. Proton MR spectra without water suppression of the volume of interest were also collected and used for correction of phase distortions due to eddy current effects.

Each eddy current–corrected spectrum was processed as follows: the time domain signal was zero-filled to 2048 points; an exponential multiplier of 4 to 6 Hz was applied to the time domain signal (the amount of linewidth broadening applied depended on the water shim obtained and typically the full width of the water signal at half maximum signal intensity was between 4 and 6 Hz); a Fourier transformation was performed to obtain the frequency domain information; the spectrum was then phase-corrected generally by using only a zero-order correction; and the baseline was corrected using a second-order spline function.

Phantom and Patients

The phantom consisted of a 500-mL polystyrene flask filled with a 0.15-N phosphate-buffered saline solution (pH 7.4) containing approximately 20 mM *N*-acetylaspartate (NAA) (chemical-shift position, 2.0 ppm), 20 mM creatine (Cr, 3.0 ppm), and 10 mM choline (Cho, 3.2 ppm). This flask was then immersed in a 1000-mL glass beaker filled with commercial vegetable oil (CH3 groups of fatty acids, 0.9 to 1.2 ppm, and CH2 groups of fatty acids, 1.3 to 1.6 ppm) (Fig 1). For each of the three volumes, three different TEs were studied with the STEAM technique using this phantom (a total of nine studies). For the PRESS sequences, two different volumes were studied using two different TEs (for a total of six studies) using the phantom. At least one side of each volume was located 2 to 4 mm from the water/oil boundary to avoid distortions in the proton MR spectra resulting from the large magnetic susceptibility differences between water/polystyrene and fat/

polystyrene interfaces. Similarly, at least one side of each volume of interest was defined 2 to 4 mm from fat-containing structures (retroorbital and subcutaneous fat of the scalp) in the volunteers.

For the human studies, three healthy volunteers were recruited. After obtaining the previously mentioned T1-weighted axial images, placement of the volumes of interest was as follows: two volumes (8 and 27 cm^3) were placed at the left frontotemporal region close to but not including any retroorbital fat; two volumes (8 and 27 cm^3) were placed in the superior aspect of the left centrum semiovale close to but not including any subcutaneous scalp fat; and two volumes (8 and 27 cm^3) were placed in the left occipital region close to but not including the subcutaneous scalp fat. Each of these three placements was examined with TEs of 135 and 270 with STEAM and PRESS sequences for a total of 24 studies per individual (more than one session per volunteer was required).

Measurement of Section Profiles

Section profiles were measured by using a custom-designed pulse sequence in which the echo was acquired in the presence of a gradient parallel to the slice-selection direction. This generated images corresponding to the volume of excitation with the slice-selection direction visible in the image. These studies were acquired with the same MR unit (mentioned previously) using the standard receive/transmit head coil and the manufacturer's phantom (170-mm defined spherical volume water phantom containing $NiSO_4$; inversion time, 310). The nonsection measurement parameters were as follows: 200 $\times$ 200-mm^2 field of view, 512 $\times$ 512 acquisition matrix, 0.39 $\times$ 0.39-mm^2 spatial resolution, 130 Hz/pixel receiver bandwidth; 1000/16,24/1, and transverse section orientation. The frequency-selective excitation pulses used for slice selection were sinc-Hanning functions truncated to 2560 microseconds. For the 180° refocusing pulse, the frequency bandwidth was broadened by 27%. The section-selection gradient for all pulses was 2.0 mT/m with the radio frequency functions calculated on the basis of the desired section thickness. The two pulse sequences used were a spoiled gradient-echo sequence that allowed for visualization of the excitation pulse profile and a spin-echo sequence in which the excitation pulse was a rectangular 90° pulse and the 180° refocusing pulse was frequency selective, allowing for visualization of the refocusing pulse profile. Two section thicknesses were chosen (2 and 4 cm), representing the two extremes of slab thickness allowed for proton MR spectroscopic studies in our system.

Data analysis was performed by evaluating a profile near the midpoint of the section and assessing the full width at half maximum height (FWHM) and at 10% of maximum height (FWTM). This was done by determining the pixel amplitudes on each side of the profile nearest the desired value (FWHM and FWTM) and calculating the corresponding distance. Since pixel amplitudes were never at exactly the desired value, the outermost of the two pixels bracketing the desired value was chosen. This ensured that the calculated thickness always exceeded the actual thickness and that the overestimation was no greater than 0.78 mm (two pixels).

Results

Phantom and Human Studies

The spectra obtained using the STEAM sequence (TE of 135) on 2 $\times$ 2 $\times$ 2-cm^3 volumes adjacent to the fat/lipid layer (Fig 2A) consistently showed peak resonances for fat (Fig 2B). In contrast, PRESS studies (TE of 135) of this volume showed extremely small fat resonances (Fig 2C). Similarly, if the volume size was increased to 3 $\times$ 3 $\times$ 3 cm^3, the amount of lipid contamination and phase distortion due to magnetic susceptibility effects of the fat/polystyrene/water interface increased when STEAM was used rather than PRESS (Fig 3). As shown in Figure 4, increasing the TE in the STEAM sequence from 20 to 135 led to a significant decrease in the amount of extraneous fat/lipid resonances observed in the 4 $\times$ 4 $\times$ 4-cm^3 volume. When the TE was increased to 270, the fat/lipid resonance in the 64-cm^3 volume was barely observable. Increasing the TE has been used as a method to decrease or suppress the presence of the fat/lipid resonance (5), which results from the shorter T1 relaxation time of the protons in fats/lipids as compared with other proton metabolites of brain, such as NAA, Cho, and Cr.

The STEAM studies in the volunteers, with a TE of 135 and volumes of 2 $\times$ 2 $\times$ 2 cm^3 or 3 $\times$ 3 $\times$ 3 cm^3, showed large fat/lipid contamination when the defined volume was placed close to the retroorbital fat (Fig 5). In the PRESS sequences, with a TE of 135, no fat/lipid resonances were present, regardless of volume size (Fig 6). Volumes of interest (8 cm^3 or 27 cm^3) located near both brain surface regions studied with either STEAM or PRESS methods showed no fat/lipid contamination (Fig 7).

Section Profile Projections

Both STEAM and PRESS sequences use 90° sinc-Hanning pulses for excitation that produce the section excitation profiles shown in Figure 8. The STEAM method uses three 90° sinc-Hanning pulses for localization, whereas the PRESS method uses one 90° and two 180° sinc-Han-

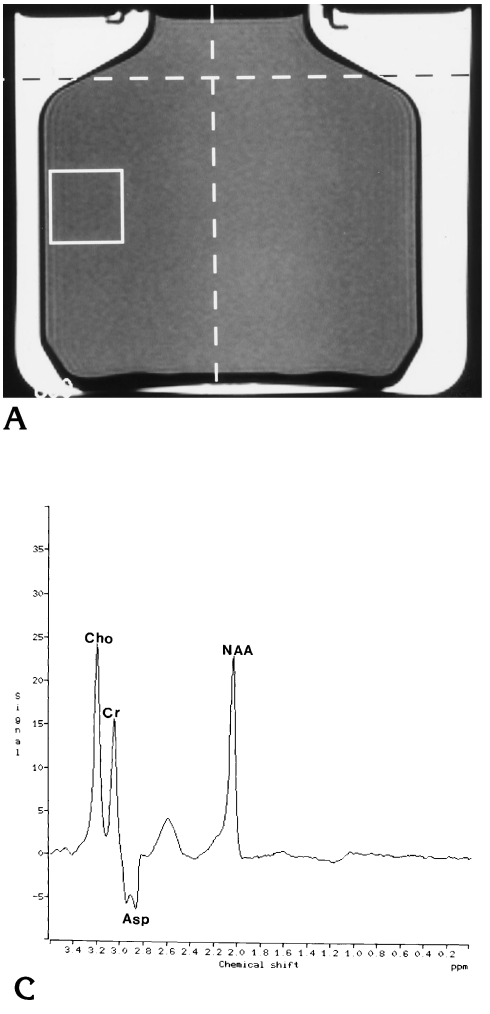

Fig 2. Phantom study using a 2 × 2 × 2-cm volume.

A, T1-weighted MR image through the phantom shows the relatively low signal of the central water compartment and high signal intensity of the peripheral fatty compartment. Note position of voxel close to but not directly encompassing fat.

B, Proton MR spectroscopy STEAM sequence (TE of 135) shows resonances corresponding to (*Lipids*) methyl and methylene groups of fatty acids (inverted peak), NAA, Cr, and Cho.

C, Proton MR spectroscopy PRESS sequence (TE of 135) shows similar resonances as in *B* but no fatty acids. Inverted resonance between 2.6 and 2.8 ppm corresponds to methylene groups of aspartate (*Asp*).

ning pulses for refocusing, which produce excitation profiles as shown in Figure 9. For the excitation pulse, the largest discrepancy between the nominal and the actual section thickness was at 2-cm thickness, where the FWHM exceeded the nominal section thickness by 14%. At 4-cm thickness, deviation from the nominal thickness was significantly less than the requested values. At the base of the excitation volume, the FWTM was greater than the nominal thickness for all pulses, with the 20-mm nominal thickness being 49% wider. The 180° refocusing pulses excited regions 13% to 21% greater than nominal.

The Table lists the regions of the excitation for a requested section thickness. Use of these data for the FWHM section profile values for the dimensions of the volumes of interest suggests that the STEAM method gives a larger than expected volume. In the case of a 2 × 2 × 2-cm^3 volume, its actual size is 2.27 × 2.27 × 2.27 cm^3, or 11.70 cm^3. Because the PRESS method uses different refocusing pulses, the defined volume is smaller. In the case of a 2 × 2 × 2-cm^3 volume, the actual size is 2.27 × 1.72 × 1.72 cm^3, or 6.71 cm^3. If the STEAM-defined volume is larger and the PRESS-defined volume is smaller, then extraneous lipid contamination in a defined volume of interest is greater when using the STEAM method. Extraneous lipid contamination in the defined volume may be further exacerbated because the FWTM (which-

Radio frequency section profile analysis

Radio Frequency Pulse Type	Nominal Section Thickness, mm	FWHM, mm	FWTM, mm
Excitation (90°)	20	22.7	29.7
Excitation (90°)	40	41.0	47.6
Refocussing (180°)	20	17.2	24.2
Refocussing (180°)	40	37.1	45.3

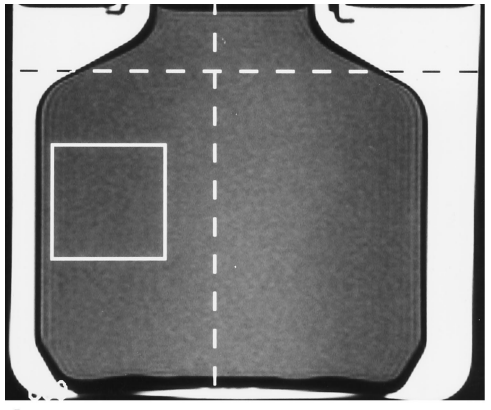

A

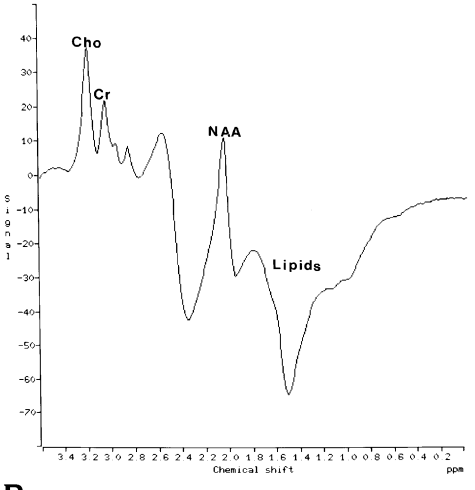

B

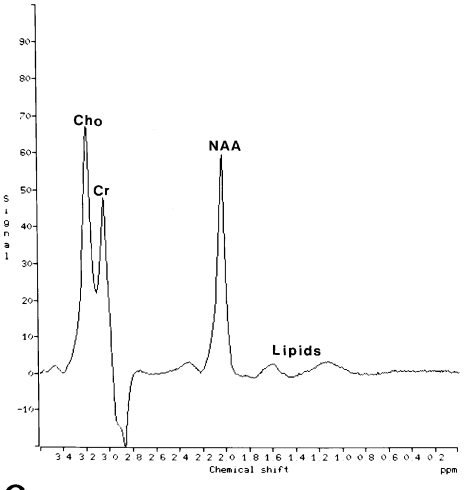

C

Fig 3. Phantom study using a 3 × 3 × 3-cm volume.

A, T1-weighted image shows position of voxel in phantom.

B, Proton MR spectroscopy STEAM sequence (TE of 135) shows resonances corresponding to fatty acids (*Lipids,* inverted peak), NAA, Cr, and Cho.

C, Proton MR spectroscopy PRESS sequence (TE of 135) shows similar resonances but very few lipids.

gives a measure of frequency ranges excited outside the defined volume of interest) is also higher for STEAM than it is for PRESS.

Discussion

In proton MR spectroscopy, one of the primary concerns is the degree of localization. For single-voxel techniques, such as STEAM and PRESS, this is mainly determined by the quality of the section profile, which depends on the hardware characteristics of the unit used. Section profile imperfections lead to saturation effects (crosstalk) between sections. In spin-echo imaging, multiple parallel radio frequency pulses excite the tissue of interest prior to signal detection. The final section profile imperfections result from a combination of imperfections, which may or may not be better than the individual pulses themselves. For spin-echo or STEAM spectroscopic techniques, in which multiple radio frequency pulses are applied orthogonal to one another, exciting the same nominal volume of tissue, section profile imperfections for all pulses must be examined when performing single-voxel MR spectroscopy. Section profile imperfections affect the total amount of tissue excitation in each direction and the total amount of contamination from adjacent tissues. Thus, misinterpretation of the proton MR spectroscopic data may occur if an estimate of these effects is unknown.

The FWHM provides a measure of the total amount of volume that is excited. Our results showed that the greatest percentage of deviation in volume occurred when the smaller volume (8 cm^3) was used, wherein the actual excited volume was 32% larger than the defined one. For our largest volume (64 cm^3), the percentage of deviation was smaller (7%). For PRESS, the defined 8-cm^3volume was smaller by 16% than the nominal one and the defined

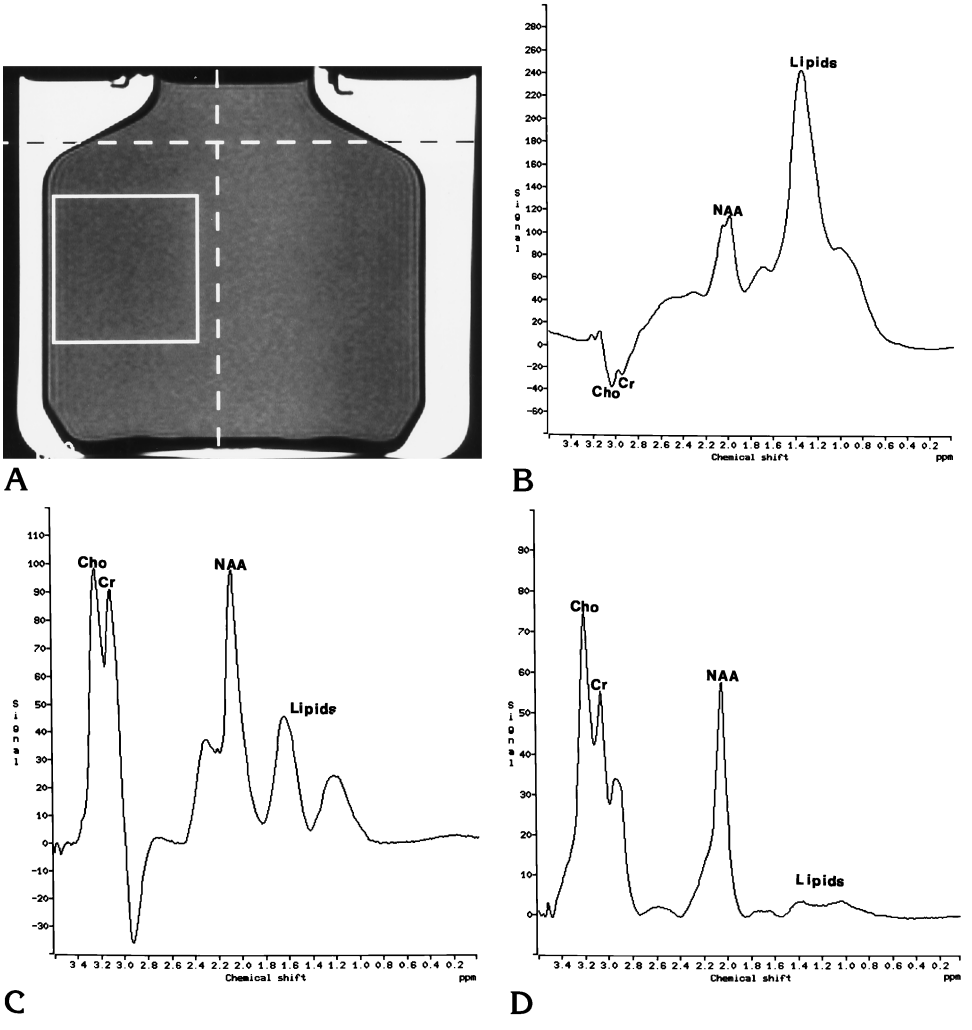

Fig 4. Experiment illustrating the effect of varying the TE on the degree of fat contamination in the voxel observed in a 4 × 4 × 4-cm volume, STEAM sequences, and repetition time of 1600.

A, T1-weighted image shows position of voxel in the phantom.

B, Spectrum at TE of 20 shows fatty acids (*Lipids*), NAA, Cr, and Cho.

C, Spectrum at TE of 135 shows fatty acids (*Lipids*), NAA, Cr, and Cho.

D, Spectrum at TE of 270 shows fatty acids (*Lipids*), NAA, Cr, and Cho. Note progressive loss of intensity of lipids with prolongation of TE in this experiment.

64-cm^3 volume was smaller by 12% than the nominal one. Our results are similar to those previously published (6). In that study, in which a 1.5-T GE Signa unit was used, the STEAM technique gave an actual volume that was 67% greater than the PRESS volume. The results of that study also suggest that the differences between the STEAM and PRESS methods may apply to more than just one MR unit. Our methods are described in detail so that similar experiments may be performed by others with MR units of different manufacturers.

Extraneous contamination is also an aspect of section profile imperfection. The FWTM provides a useful measure of the extent of contamination arising outside a defined volume of interest. As we have shown, the greatest amount of contamination occurred with the STEAM sequences. Our results differ from those of Yongbi et al (2), who used a Siemens 1.5-T GBS1 MR unit and found that extraneous contamination was higher with PRESS (7% to 12%) than with STEAM (3% to 8%). The differences between their study and ours may be attributable in part to the pulse generators used to define the shape of the frequency section-selective pulses. In the Siemens GBSI system, the pulse generator uses 256 complex data points to define the shape of the pulse, whereas the Siemens SP4000 pulse generator uses 512 complex data points. This should lead to a much better section profile in the Siemens SP 4000, because the shape of the pulse is better defined. Additionally, their unit was equipped with a Hamming filter rather than with the Hanning filter used in our unit, which may also have contributed to the differences observed in this study, since these filters are used to truncate the sinc functions. Therefore, it appears that extraneous lipid contamination may be dependent on the MR unit and that

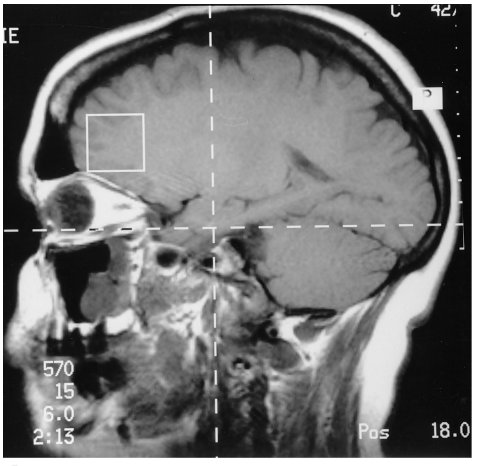

A

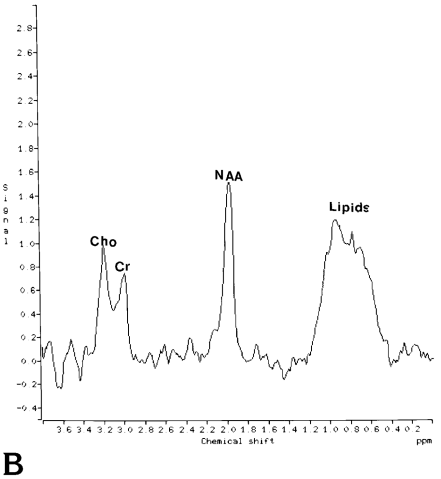

B

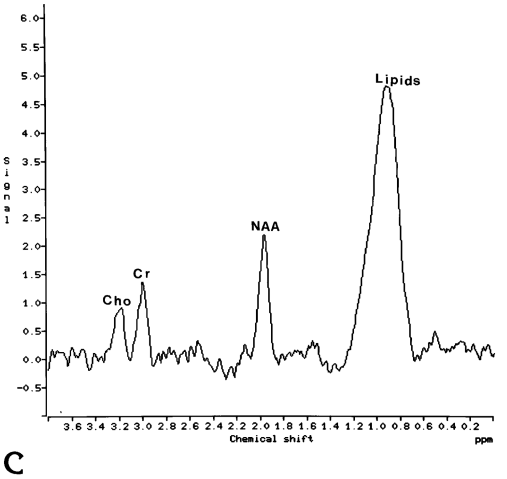

C

Fig 5. Proton MR spectroscopy of human brain adjacent to retroorbital fat (STEAM: TE of 135, repetition time of 1600).

A, Parasagittal T1-weighted image shows position of the voxel.

B, Spectrum of 2 × 2 × 2-cm volume shows lipids, NAA, Cr, and Cho.

C, Spectrum of 3 × 3 × 3-cm volume shows more lipids than in *B* and also NAA, Cr, and Cho.

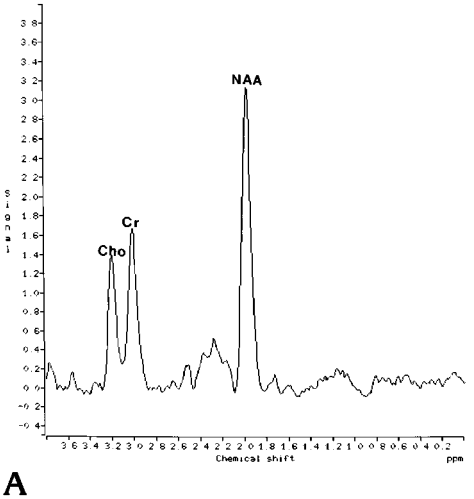

A

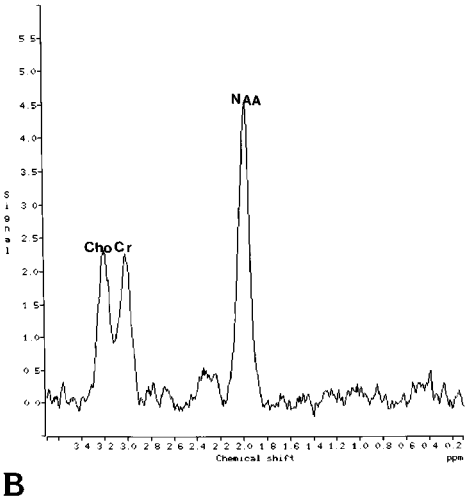

B

Fig 6. Proton MR spectroscopy of human brain adjacent to retroorbital fat (PRESS: TE of 135).

A, Spectrum of 2 × 2 × 2-cm volume (identical to that in Fig 4B) shows NAA, Cr, and Cho, but no obvious lipids.

B, Spectrum of 3 × 3 × 3-cm volume shows NAA, Cr, and Cho. Note absence of extraneous lipid contamination in both studies.

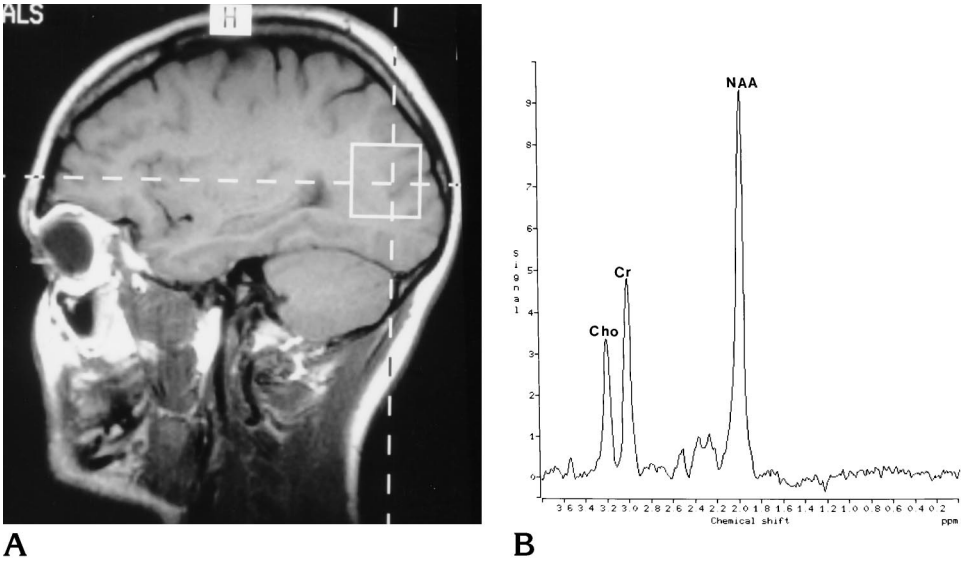

Fig 7. Proton MR spectroscopy of human brain with voxel near subcutaneous scalp fat.

A, Parasagittal T1-weighted MR image shows position of voxel.

B, Spectrum (STEAM: TE of 135, 3 × 3 × 3 cm) shows NAA, Cr, and Cho, but no lipid contamination.

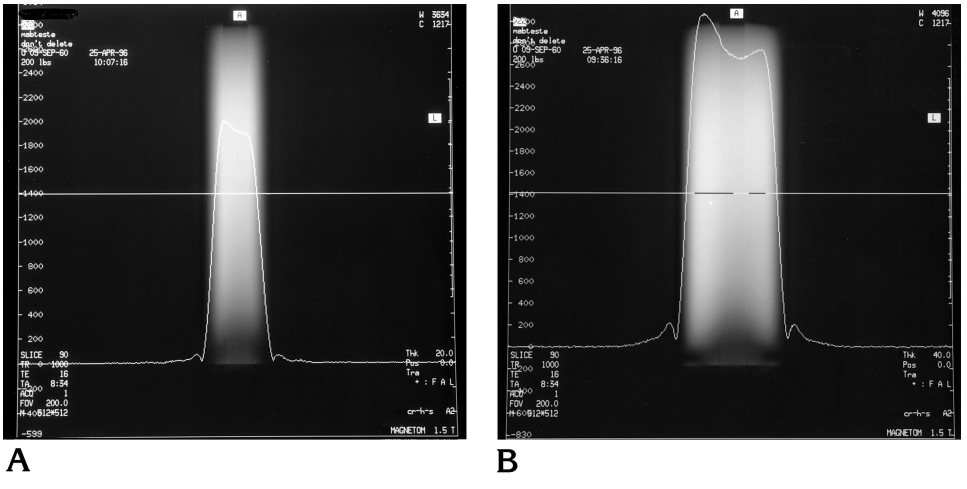

Fig 8. Section profile projections for the 90° sinc-Hanning excitation pulses.

A, Profile for a 2-cm defined section.

B, Profile for a 4-cm defined section.

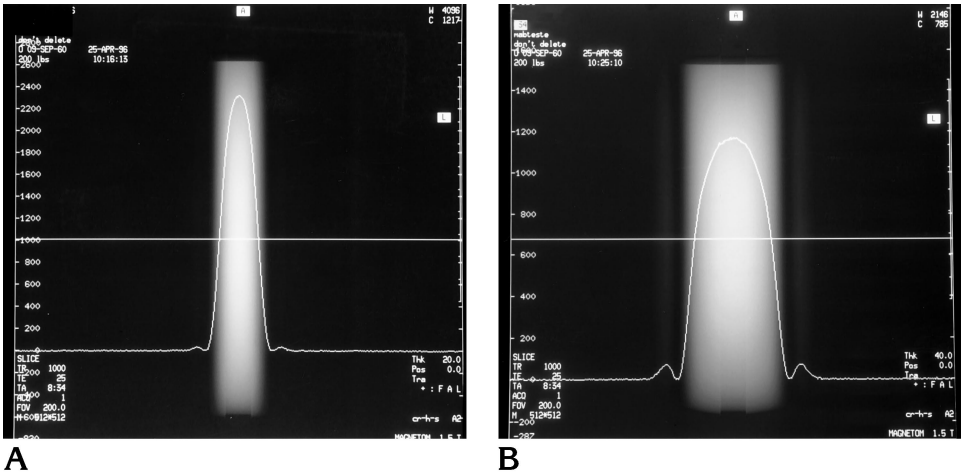

Fig 9. Section profile projections for the 180° sinc-Hanning refocusing pulses.

A, Profile for a 2-cm defined section.

B, Profile for a 4-cm defined section.

experiments such as ours are needed if one wishes to establish individual degrees of extraneous lipid contamination.

Differences in the actual size of selected volumes are clinically important when performing proton MR spectroscopy with either STEAM or PRESS sequences, particularly when interpretation of the presence of lipids is required. For example, presence of lipids in an intraaxial mass may reflect necrosis, and therefore, a higher grade of malignancy. Lipids are present in glioblastoma multiforme (7, 8). Some extraaxial masses, such as meningiomas, may also contain lipids (8). The presence of lipids in a previously irradiated mass may signify radiation necrosis (9, 10). The appearance of lipid resonances has been associated with the inflammation that occurs in the early stages of multiple sclerosis plaque evolution (11). If contamination from extraneous lipids is present in any of these situations, an erroneous interpretation of the proton MR spectroscopic data may occur. On the basis of our results, one may expect greater contamination from extraneous lipids when using STEAM sequences. In our experience, this technique is desirable when analyzing smaller regions of the brain, such as the hippocampi, the brain stem, or tumors close to the cortex. In our system, the standard manufacturer's software presently only allows STEAM sequences in the examination of volumes less than 8 cm^3. In brain structures close to the skull and its base, contamination by lipids from bone marrow or subcutaneous tissue becomes an issue. Placement of the volume of interest as far away as possible from these potential lipid-containing sources is prudent to avoid contamination. Fat-saturation pulses also provide a means of diminishing lipid contamination but may reduce the signal of intrinsic lipids. If the area to be examined allows for larger volumes of interest, prolongation of the TE also helps to diminish the intensity of contaminating lipid resonances but reduces the signal from many other metabolites.

In summary, in our experiment, the STEAM localization method with a short TE (20 milliseconds) resulted in the greatest amount of extraneous lipid contamination. The intensity of contaminant lipids decreased by prolonging the TE to 270. When the STEAM technique was applied to human studies, significant lipid contamination was seen when the voxel was defined close to the retroorbital fat but was not affected by proximity to the subcutaneous scalp fat. The PRESS localization method in our MR system did not result in any significant extraneous lipid contamination regardless of its position, size, and TE in either the phantom model or the volunteers.

References

1. Haupt CI, Schuff N, Weiner MW, Maudsley AA. Removal of lipid artifacts in ^1H spectroscopic imaging by data extrapolation. *Magn Reson Med* 1996;35:678–687
2. Yongbi NM, Payne GS, Collins DJ, Leach MO. Quantification of signal selection efficiency, extra volume suppression, and contamination for ISIS, STEAM, and PRESS localized ^1H NMR spectroscopy using an EEC localization test object. *Phys Med Biol* 1995;40:1293–1303
3. Frahm J, Bruhn H, Gyngell M, Merboldt K, Haenicke W, Sauter R. Localized high resolution proton NMR spectroscopy using stimulated echoes: initial applications to human brain in vivo. *Magn Reson Med* 1989;9:79–93
4. Bottomley P. Spatial localization in NMR spectroscopy in vivo. *Ann N Y Acad Sci* 1987;508:333–340
5. Campbell ID, Dobson CM, Williams RJP, Wright PE. Pulse methods for the simplification of protein NMR spectra. *FEBS Lett* 1975; 57:96–99
6. Moonen CTW, von Kielin M, van Zijl PCM. Comparison of single-shot localization methods (STEAM and PRESS) for in vivo proton NMR spectroscopy. *NMR Biomed* 1989;2:201–208
7. Negendank WG, Sauter R, Brown TR, et al. Proton magnetic resonance spectroscopy in patients with glial tumors: a multicenter study. *J Neurosurg* 1996;84:449–458
8. Kuesel A, Sutherland G, Halliday W, Smith I. ^1H MRS of high grade astrocytomas: mobile lipid accumulation in necrotic tissue. *NMR Biomed* 1994;7:149–155
9. Castillo M, Kwock L, Mukherji SK. Clinical applications of proton MR spectroscopy. *AJNR Am J Neuroradiol* 1996;17:1–15
10. Kugel H, Heindel W, Ernestus RI, Bunke J, du Mesnil R, Friedman G. Human brain tumors: spectral patterns detected with localized H-1 NMR spectroscopy. *Radiology* 1992;183:701–709
11. Narayama PA, Wolinsky JS, Jackson EF, McCarthy M. Proton MR spectroscopy of gadolinium-enhanced multiple sclerosis plaques. *J Magn Imaging 1992;2:263–270*